An Improved Spacetime Ray Tracing System for the Visualization of Relativistic Effects

Jiang Li, Heung-Yeung Shum

Microsoft Research, China

{jiangli, hshum}@microsoft.com

Qunsheng Peng

State Key Lab of CAD&CG, Zhejiang Univ.

peng@cad.zju.edu.cn

Abstract

Traditional ray tracing methods are based on Newton's classical mechanics. They cannot reproduce the visual phenomena of high-speed motion. In this paper, we develop an improved spacetime ray tracing system, which provides a framework for the visualization of spacetime relativistic effects. The system consists of three major components. First, a transformation platform is established to process the transformations of spacetime coordinates and velocities between different scene elements. This enables the independent scene modeling at different reference frames. Second, a number of spacetime scene data structures are constructed to encapsulate conventional scene elements such as objects, light sources, and cameras. Third, a medium information stack is designed to record in which medium the tracing ray is traveling. This enables the accurate calculations of light speeds, which are critical in the visualization of relativistic effects. Experiments are performed when synthetic objects, light sources and cameras are moving at high speeds relative to each other. In addition to conventional relativistic effects, we discover in our system a number of novel visual effects such as multiple transmissions, omnidirectional reflection, and delayed appearance of shadows.

1. Introduction

Traditional ray tracing methods[18] are based on Newton's classical mechanics. These methods assume that the speeds of objects are so slow that the delays in the flight of light between scene elements can be ignored. With the use of these kinds of algorithms, spacecraft traveling at light speed are displayed no differently in computer-generated science fiction movies. According to the special theory of relativity, the measurements and appearances of objects are closely related to the motions of the observers. Specifically, the shapes of high-speed objects should be distorted or rotated due to the length contraction effect and the spectra of light should also be shifted if they are measured or observed in a high-speed reference frame.

The invention of the computer and the development of graphic technologies provide humans with opportunities to experience relativistic effects virtually. Hsiung et.al.[10] proposed a special ray tracing method to describe relativistic effects in spacetime. In the REST-frame algorithm[3, 4, 5], objects, light sources and cameras resting at different inertial reference frames are modeled. Tracing rays are in turn transformed to different inertial reference frames, then intersection tests and light illumination calculations are performed. As results, a series of phenomena such as length contraction, time dilation[9] and Doppler shift effect[7, 8] have been visualized. Shading of high-speed moving objects was also studied via transforming all the objects and light sources to the inertial reference frame of the camera[2, 6, 13]. A fast rendering algorithm was proposed, which incorporated the above approaches and could simulate multiple independently moving objects and animations[1]. In addition, an image-based approach was utilized to render high speed flights through real-world scenes filmed by standard cameras[16].

However, there are several main problems in the previous methods. First, previous methods assume that all the axes of scene coordinate systems in different reference frames are aligned with each other. This is impractical for synthetic modeling. As scenes at different reference frames may need to be modeled independently, it will be convenient if their relationships can be connected by a few parameters that are isolated from the modeling process. We will define such a set of parameters in Section 3.1. Second, in previous methods, most of the scene data structures are

still in 3D status and are time insensitive, therefore (1) changes in object appearances in animations cannot be represented; (2) the movement or properties of some scene elements are usually constrained, e.g. the light sources are usually assumed to be isotropic point and be stationary in the object frame. Finally, the light rays are always assumed to travel in a vacuum. Actually, they may travel in various media such as air, glass, or water in different time intervals. Since the delay of light flight relies strongly on the speed of light, it is crucial to determine the traveling medium in the ray tracing process. Due to the above limitations, previous methods cannot produce transmission and reflection phenomena, and cannot efficiently generate shadow.

It should be noted that this paper only considers the spacetime part of relativistic effects. The detailed discussion on the relativistic Doppler effects can be found in references[2, 7, 8, 17].

The remainder of this paper is organized as follows. In Section 2, we review the background of special relativity. Section 3 describes the framework that provides improved spacetime ray tracing. Some novel visual effects such as multiple transmission, omnidirectional reflection and delayed appearance of shadows are shown in Section 4. Finally we conclude our work and discuss future directions in Section 5.

2. The Background of Special Relativity

Albert Einstein established the Special Theory of Relativity in 1905 upon the following two postulates[11, 12, 14]:

- Non-existence of preferred reference system: the laws of physics must be the same for observers in all inertial reference systems.

- Constancy of speed of light: c is constant in a vacuum in all inertial frames and is independent of the motion of a light source relative to the observer.

Accordingly, some rules are deduced:

- The measured space and time coordinates are dependent upon the reference frame from which the measurement is conducted.

- The Lorentz Transformation equations relate measured spacetime coordinates between inertial reference frames, and therefore:

  - Lengths perpendicular to relative motion are constant regardless of the inertial observer.

  - Lengths parallel to relative motion are measured to have undergone contraction in comparison with their rest lengths.

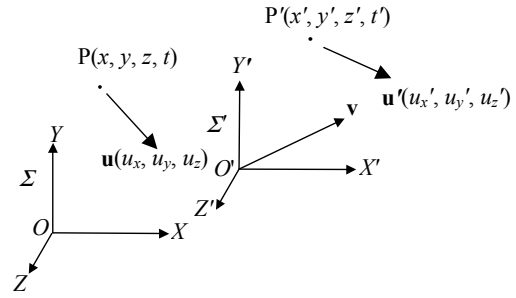 - Clocks in inertial frames have varying rates dependent upon their motions.

Figure 1: *Spacetime and velocity relationships between two inertial reference frames.*

As shown in Figure 1, suppose that there are two initial reference frames Σ and Σ'. Σ' is moving relative to Σ with velocity $\mathbf{v} = (v_x, v_y, v_z)$. We call Σ the inertial reference frame of the ground and Σ' the inertial reference frame of, for instance, a space shuttle. Without loss of generality, the coordinate systems in Σ and Σ' are so chosen that their axes are parallel to each other and their origins O' and O also coincide with each other at time $t = t' = 0$. An event occurs at a position $\mathbf{P'}$ at time t' measured in Σ' can be described by a spacetime coordinate $P' = (\mathbf{P'}, t') = (x', y', z', t')$. Its corresponding spacetime coordinate $(\mathbf{P}, t)$ measured in Σ is related to $(\mathbf{P'}, t')$ via Lorentz Transformation[11]

$$\mathbf{P} = \mathbf{P'} + \left[\frac{(\gamma-1)}{v^2}(\mathbf{P'} \bullet \mathbf{v}) + \gamma t' \right]\mathbf{v}, \quad t = \gamma\left(t' + \frac{\mathbf{P'} \bullet \mathbf{v}}{c^2} \right) \quad (1)$$

where

$$\gamma = 1 \Big/ \sqrt{1 - \frac{v^2}{c^2}}, \quad v =\parallel \mathbf{v} \parallel = \sqrt{v_x^2 + v_y^2 + v_z^2} \quad (2)$$

Suppose that the velocity of an object measured in Σ' is $\mathbf{u'}(u_x', u_y', u_z')$, then the velocity $\mathbf{u}(u_x, u_y, u_z)$ of the same object measured in Σ is related to $\mathbf{u'}(u_x', u_y', u_z')$ via the Lorentz velocity transformation[11]

$$\mathbf{u} = \left[\mathbf{u'} + \left(\frac{\gamma-1}{v^2}\mathbf{v} \bullet \mathbf{u'} + \gamma \right)\mathbf{v} \right] \Big/ \left[\gamma\left(1 + \frac{\mathbf{v} \bullet \mathbf{u'}}{c^2} \right) \right] \quad (3)$$

If the quantities in the inertial reference frame Σ is known and we want to deduce the quantities in the inertial reference frame Σ', the formulas are symmetric except that $\mathbf{v}$ is replaced by -$\mathbf{v}$.

3. An Improved Spacetime Ray Tracing Framework

3.1 A platform of spacetime transformation

In the synthetic modeling of space flights, the measurements are usually established in the local coordinate system of each space shuttle or scene elements. It is better define a set of parameters for establishing the

spacetime relationships between different space shuttles or scene elements. In the following we will explore an optimum description of the spacetime relationship between different space shuttles or scene elements that are located in different reference frames.
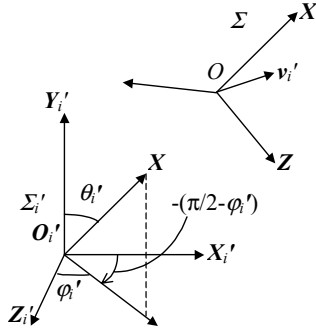

Figure 2: *Assume that there exist two reference frames Σ and Σ_i'. Σ is moving with velocity v_i' relative to Σ_i'.*

As illustrated in Figure 2, assume that there exist two reference frames Σ and Σ_i'. Σ represents the inertial reference frame of the ground, and Σ_i' represents one of the inertial reference frames of objects, light sources or cameras. Σ is moving with velocity v_i' relative to Σ_i'. The coordinate systems of different reference frames may not be aligned with each other. In order to align the axes of the two coordinate systems, we apply some operations of translation and rotation on the coordinate system of Σ_i'.

Suppose that the orientation angles of the X axis of the coordinate system of Σ are measured as (θ_i', φ_i') in Σ_i'. If the origin of the coordinate system $X_i'Y_i'Z_i'$ in Σ_i' is translated to the origin of the coordinate system XYZ in Σ and rotated around its $Y_i(=Y_{i1}')$ axis by an angle of $[-(\pi/2-\varphi_i')]$, an arbitrary point $P_i' = (P_{ix}', P_{iy}', P_{iz}', P_{it}')^T$ in $X_i'Y_i'Z_i'$ becomes P_{i1}' in $X_{i1}'Y_{i1}'Z_{i1}'$, where $X_{i1}'Y_{i1}'Z_{i1}'$ is the translated and rotated coordinate system of $X_i'Y_i'Z_i'$.

$$P_{i1}' = M_{i1}'(P_i' - P_{i0}') \qquad (4)$$

where $P_{i0}' = (P_{i0x}', P_{i0y}', P_{i0z}', P_{i0t}')$ is the spacetime coordinate of the origin of XYZ measured in Σ_i', M_{i1}' is the corresponding spacetime rotation matrix, in which the space part undergoes a standard rotation transformation and the time part remains unchanged. Note the time axis is not shown in Figure 2.

If the coordinate system $X_{i1}'Y_{i1}'Z_{i1}'$ is rotated around its Z_{i1}' $(=Z_{i2}')$ axis by an angle of $(\pi/2-\theta_i')$, the spacetime coordinate of P_{i1}' in $X_{i1}'Y_{i1}'Z_{i1}'$ becomes P_{i2}' in $X_{i2}'Y_{i2}'Z_{i2}'$, where $X_{i2}'Y_{i2}'Z_{i2}'$ is the rotated coordinate system of $X_{i1}'Y_{i1}'Z_{i1}'$.

$$P_{i2}' = M_{i2}'P_{i1}' \qquad (5)$$

where M_{i2}' is the corresponding spacetime rotation matrix. Now the X_{i2}' axis has been aligned with the X axis.

After these two rotation operations, the Y_{i2}' or Z_{i2}' axis of the coordinate system $X_{i2}'Y_{i2}'Z_{i2}'$ in Σ_i' may precede to the Y or Z axis of the coordinate system XYZ in Σ by an angle of ω_i'. We further apply a rotation operation to $X_{i2}'Y_{i2}'Z_{i2}'$ so that the new coordinate system $X_{i3}'Y_{i3}'Z_{i3}'$ is aligned with XYZ. Accordingly, the P_{i2}' in $X_{i2}'Y_{i2}'Z_{i2}'$ becomes P_{i3}' in $X_{i3}'Y_{i3}'Z_{i3}'$

$$P_{i3}' = M_{i3}'P_{i2}' \qquad (6)$$

where M_{i3}' is the corresponding spacetime rotation matrix. Now we can connect the spacetime coordinates of the same point in $X_{i3}'Y_{i3}'Z_{i3}'$ and XYZ by Eq.(1) (in which $\mathbf{v} = -\mathbf{v_i}$). We have

$$P_i = M_{iL}'M_{i3}'M_{i2}'M_{i1}'(P_i' - P_{i0}') \qquad (7)$$

where P_i is the spacetime coordinate of the point measured in XYZ of Σ, and M_{iL}' is the equivalent matrix expression of Eq.(1). For velocities, we have

$$\mathbf{u_i} = F_{iL}'(M_{i3}'M_{i2}'M_{i1}'\mathbf{u_i}') \qquad (8)$$

where $\mathbf{u_i}'$ is the velocity vector of an object measured in $X_i'Y_i'Z_i'$ of Σ_i', $\mathbf{u_i}$ is the velocity vector of the same object measured in XYZ of Σ, and F_{iL}' denotes the function representing Eq.(3). Note $\mathbf{u_i}'$ and $\mathbf{u_i}$ should be expressed in homogenous coordinates since they are originally in 3 dimensions.

As we can see, the spacetime relationship between the coordinate systems of two reference frames is defined by three parameters, i.e. the spacetime distance $P_{i0}' = (P_{i0x}', P_{i0y}', P_{i0z}', P_{i0t}')$, the set of aligning rotation angles $(\theta_i', \varphi_i', \omega_i')$, and the relative velocity $\mathbf{v_i}$. With the use of above definition, each reference frame only need measure its set of parameters with respect to the reference frame of the ground. The spacetime relationship between each pair of reference frames can be established via the reference frame of the ground.

3.2 4D scene data structures

In order to make the modeling and rendering of 4D scenes easy and practical, we construct a new group of 4D scene data structures that are used to encapsulate the conventional scene data structure:

(1) Scene structure

It includes all the data structures in the scene, such as reference frame, camera, object, light source, material, and texture data structures.

(2) Reference frame structure

It contains three parameters, which define the spacetime relationship between this reference frame and the global reference frame.

(3) Medium information structure

It contains a pointer to environmental objects (such as air) or scene objects (such as glass objects) that a ray may transmit. It is used to record in which medium the camera, the object, or the light source is immersed, or the virtual ray is traveling. It is important since the light speed is inversely proportional to the refractive index of the medium.

(4) Object, camera and light source data structures

Besides conventional data structures, each of the object, the camera and the light source data structures contains a pointer to its inertial reference frame and a medium information stack to record which medium it stays. All the parameters of an object, a camera and a light source are functions of time.
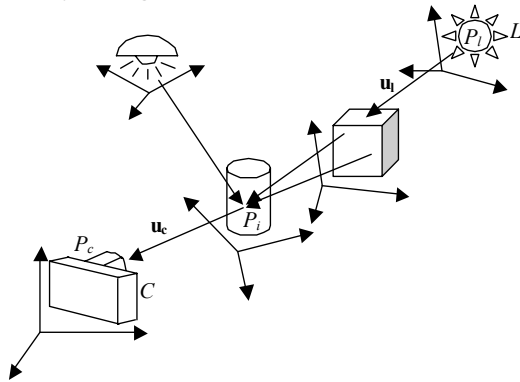
3.3 Ray tracing

Figure 3: *An illustration of the procedures of relativistic ray tracing.*

(1) Intersection test

As shown in Figure 3, the light ray that corresponds to a pixel in the image plane of camera C can be represented by a spacetime point $P_c=(\mathbf{P_c}, t_c)$ and a vector $\mathbf{u_c}$, which means that the light ray reaches the lens optical center of camera $\mathbf{P_c}$ at time t_c with velocity $\mathbf{u_c}$. According to Eqs.(7) and (8), P_c and $\mathbf{u_c}$ are transformed from the reference frame of camera C to the reference frame of the ground and then in turn to the reference frame of each object for intersection tests. After all the spacetime intersection points are transformed to the reference frame of the ground, the point with the latest time is chosen to be the visible point P_i. Note the light source can be any type rather an isotropic point as in previous methods.

(2) Light source

P_i is transformed to the reference frame of each light source. The spacetime emission point P_l and emission velocity $\mathbf{u_l}$ are determined after taking into account the flight time of the light from the light source to the visible point.

(3) Shadow detection

Each pair of P_l and $\mathbf{u_l}$ is transformed to the reference frame of each object for shadow detection. All the spacetime occlusion points and transparencies are recorded.

(4) Illumination

A light ray from P_l with velocity $\mathbf{u_l}$ passes through all the transparent occlusion points in turn with the consideration of refractive index in each medium.

(5) Local illumination

Conventional local illumination models are applied to determine the color of the visible point under the above illumination.

(6) Transmission and reflection

If there are transmissions or reflections at the visible point, recursive ray tracing is employed.
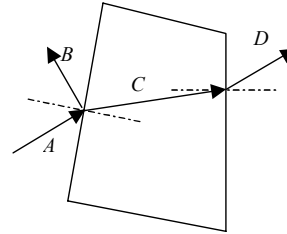
Figure 4: *A medium information stack is used to track in which medium the ray is traveling.*

It is worth mentioning that we establish a medium information stack to track in which medium a ray is traveling. When a ray is backward traced from a camera, its medium information stack is copied from that of the camera. If the ray is reflected by a surface, its medium information stack remains unchanged as shown in path *AB* in Figure 4. If the ray is refracted, we need to check the medium information item at the top of the stack. If the object pointer stored in the medium information item at the top of the stack is different from the object pointer of the current surface, it means that the ray is entering a new medium as shown in path *AC* in Figure 4. When we calculate the refraction angle, the refractive index of the incident light should be that of the object in the medium information item at the top of the stack, and the refractive index of the refracted light should be that of the current object. After that, we push an item of medium information of the current object to the stack. If the object pointer stored in the medium information item at the top of the stack is identical to the object pointer of the current surface, it means that the ray is leaving a medium as shown in path *CD* in Figure 4. We pop the top medium information item from the stack. When we calculate the refraction angle, the refractive index of the incident ray should be that of the

current object, and the refractive index of the refracted ray should be that of the object with its pointer stored in the medium information item at the new top of the stack. When we calculate the duration of light flight between different scene elements, the light speed should be equal to the speed of light in a vacuum divided by the refractive index of the medium in which the ray is traveling. In our system, all objects have certain volume. Objects with single face are forbidden.

4. Results and Discussions

We have implemented our improved spacetime ray tracing system in a Pentium III 500 workstation under Windows 2000 Professional operation system. For a scene consists of about 1000 polygons, it costs about 10 seconds to render a frame with a resolution of 640×480 pixels.

(1) Transmission phenomenon

In order to determine which parts of the environment are transmitted or reflected by a high-speed moving object, we design a virtual test room. In this room, the light source is put at the far right side of the viewer. The roof and floor are painted with patterns in different colors. The front, back, left and right walls of the room are mapped with red, green, blue, and yellow letters respectively. The letters are in alphabetical order, and play the role of a coordinate system.

Figure 5 (a) shows one frame of a video clip in which a glass cube is moving laterally from left to right at 99% of the speed of light (see the last page of the paper). We can see that the cube shows a strong sign of contraction. It seems to be rotated by an angle. The rotation phenomenon has been theoretically predicted by Terrell in 1959[15]. It occurs because the speed of the glass cube is so high that the rays emitted early from the rear part of the glass cube reaches the camera at the same time as the rays emitted later from the front part of the glass cube. These rays form an image of a rotated cube. In addition, we can see that the blue letters of the left wall are transmitted onto the front of the cube, and the green letters of the back wall are reflected on the back face of the cube due to the total reflection of light within the cube. Moreover, some red letters transmitted from the side face of the cube are identical to some letters in the left part of the front wall. The reason is that since the speed of light in glass is slower than that in a vacuum, the rays traveling through the glass will consume extra time than others. This phenomenon has not been explored by previous relativistic ray tracing. It is only realized with the use of our medium information stacks.

As shown in Figure 5 (b), a glass cube is moving towards the observer at 90% of the speed of light. The four sides of the cube are strongly protruded. Like a convex lens, the cube enlarges the red letters of the front wall. In addition, we also see some reversed letters due to the total reflection of the light in the cube.

As illustrated in Figure 5 (c), a glass cube is moving away from the observer at 99% of the speed of light. In contrast to Figure 5 (b) the cube, like a concave lens, reduces the red letters of the front wall.

(2) Reflection phenomenon

In Figure 6 (a), a polished metal cube is moving laterally from left to right at 99% of the speed of light. Similar to the cases of transmission, the cube is contracted and seems to be rotated by an angle. The green letters from the back wall are reflected by the front of the cube and the blue letters of the left wall are reflected by the left side of the cube. The reflected blue letters are enlarged because the left side of the cube has become a concave mirror. This phenomenon is usually ignored in non-reflection cases in conventional methods. One may wonder why the glass cube moving laterally from left to right in Figure 5 (a) does not become a concave lens and change the size of the red letters as well. The reason for this is that the left side and the right side of the glass cube have almost the same curvatures, therefore no enlarging or reducing effects occur.

In Figure 6 (b), a polished metal cube is moving towards the observer at 90% of the speed of light. As in the case of transmission, the four sides of the cube are protruded. The cube, like a convex mirror, not only reflects the back wall which is in front of the cube but also reflects the roof, the floor, the left wall, the right walls, and even part of the front wall, which is in the back of the cube. We call this reflection phenomenon omnidirectional reflection of high-speed moving object.

In Figure 6 (c), a polished metal cube is moving away from the observer at 99% of the speed of light. Like a concave mirror, the front of the cube reflects and enlarges the green letters of the back wall.

Some careful readers may have noticed that there are two white margins (one at the top and one at the left) in the left face of the cube in Figure 6 (a), and there are also two white margins (one at the top and one at the right) in the front face of the cube in Figure 6 (c). The reason is that the light source is located at the far right side of the observer. The top and left white margins in Figure 6 (a) and the top and right white margins in Figure 6 (c) represent the areas on the wall that are directly illuminated by the light source, whereas the remaining parts represent the shadow area cast by the metal cube itself in the past.

We have rendered 6 video clips, which are located in http://research.microsoft.com/~jiangli/eg2001demo.htm. In the demos, we compare the objects in conventional and high-speed motions side by side. In addition to the phenomena explored above, one can see apparent delayed appearance of shadow, e.g. in the video clips corresponding to the scenes of Figures 5 (b), (c) and Figures 6 (b), (c) the shadow of the cube still exists even after the cube has moved out of the wall.

5. Conclusions

In this paper, we have developed an improved spacetime ray tracing system, which provides a framework for the visualization of space-time relativistic effects. First, we define three parameters to connect the spacetime relationship between the coordinate systems of two reference frames, which are P'_0, the spacetime distance between the origins of coordinate systems, (θ', φ', ω'), the aligning rotation angles, and **v**, the relative velocity between two reference frames. Given any spacetime point or velocity vector in one reference frame, we can obtain the spacetime coordinate or velocity vector in the other reference frame with the use of matrices and functions depending on these three parameters. Our system makes the independent and interactive modeling of scenes in different reference frames possible, therefore it can cooperate with conventional modeling methods in the modeling of relativistic scenes. Second, we construct a group of spacetime scene data structures, which are used to encapsulate conventional scene data structures such as objects, light sources, and cameras. Third, we design a medium information stack, which is used to record in which medium the tracing ray is traveling. Since the flight time of light depends on the speed of light, the determination of medium is crucial in the visualization of relativistic effects. As results, we demonstrate various interesting phenomena including multiple transmission, omnidirectional reflection, and delayed appearance of shadows.

Future work may include the study of accelerated motion, motion along a curve, collision detection between objects at different referent frames.

Acknowledgements

References

1. C. Betts, "Fast Rendering of Relativistic Objects, *The Journal of Visualization and Computer Animation*, Vol.9, No.1, pp.17-32, 1998. 1

2. Meng-Chou Chang, Feipei Lai, and Wei-Chao Chen, Image Shading Taking into Account Relativistic Effects, *ACM Transactions on Graphics*, Oct. 1996, Vol.15, No.4, pp.265-300. 1, 2

3. Ping-Kang Hsiung and Robert H. P. Dunn, Visualizing Relativistic Effects in Spacetime, *Proceedings of Supercomputing'89 Conference*, 1989, pp.597-606. 1

4. Ping-Kang Hsiung, Robert H. Thibadeau, and Robert H. P. Dunn, Ray-Tracing Relativity, *Pixel*, Jan./Feb. 1990, pp.10-18. 1

5. Ping-Kang Hsiung and Robert H. Thibadeau, Spacetime Visualization of Relativistic Effects, *Proceedings of the 1990 ACM Eighteenth Annual Computer Science Conference*, Washington, DC, Feb. 1990, ACM, New York, pp.236-243. 1

6. Ping-Kang Hsiung, Robert H. Thibadeau, and Michael Wu, T-Buffer: Fast Visualization of Relativistic Effects in Spacetime, *Proceedings of the 1990 Symposium on Interactive 3D Graphics*, 1990, pp.83-88. 1

7. Ping-Kang Hsiung, Robert H. Thibadeau, Christopher B. Cox, and Robert H. P. Dunn, Doppler Color Shift in Relativistic Image Synthesis, *Proceedings of the International Conference on Information Technology*, Tokyo, Japan, Oct. 1990, pp.369-377. 1, 2

8. Ping-Kang Hsiung, Robert H. Thibadeau, Christopher B. Cox, Robert H. P. Dunn, Paul Andrew Olbrich, and Michael Wu, Wide-Band Relativistic Doppler Effect Visualization, *Proceedings of the Visualization'90 Conference*, Oct. 1990, pp.83-92. 1, 2

9. Ping-Kang Hsiung, Robert H. Thibadeau, Christopher B. Cox, and Robert H. P. Dunn, Time Dilation Visualization in Relativity, *Proceedings of Supercomputer'90 Conference*, Nov. 1990, pp.835-844. 1

10. Ping-Kang Hsiung, *Visualizing Relativistic Effects*, Ph.D. thesis, Department of Electrical and Computer Engineering, Carnegie Mellon Univ., Pittsburgh, Penn, Nov. 1990. 1

11. C. Møller, *The Theory of Relativity*, Oxford University Press, 1960. 2

12. Robert Resnick, *Introduction to Special Relativity*, Rensselaer Polytechnic Institute, 1968. 2

13. C.M. Savage and A.C. Searle, Visualising Special Relativity, *The Physicist*, Vol. 36, P.141, July/August 1999. 1

14. E. Taylor and J. Wheeler, *Spacetime Physics*, MIT/Princeton, 1966. 2

15. James Terrell, Invisibility of the Lorentz Contraction, *Physics Review*, Nov. 1959, Vol.116, No.4, pp.1041-1045. 5

16. Daniel Weiskopf, Daniel Kobras, and Hanns Ruder, Real-World Relativity: Image-Based Special Relativistic Visualization, *IEEE Visualization 2000 Proceedings*, T. Ertl, B. Hamann, A. Varshney (eds.), ACM Press, October 2000, 303-310. 1

17. Daniel Weiskopf, Ute Kraus, and Hanns Ruder, Searchlight and Doppler Effects in the Visualization of Special Relativity: A Corrected Derivation of the Transformation of Radiance, *ACM Transactions on Graphics*, Vol.18, No.3, Pages 278-292, July, 1999. 2

18. Turner Whitted, An Improved Illumination Model for Shaded Display, *Communications of the ACM*, Jun. 1980, Vol.23, No.6, pp.343-349. 1
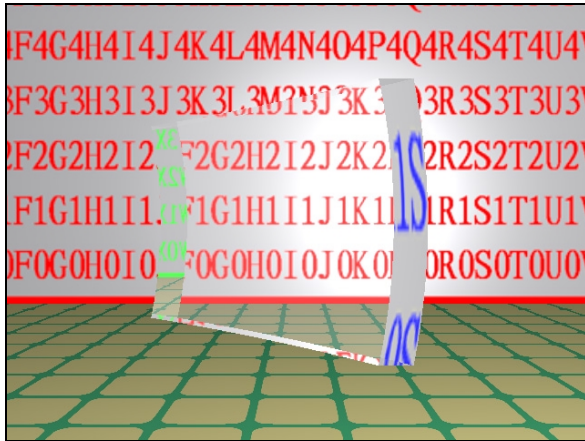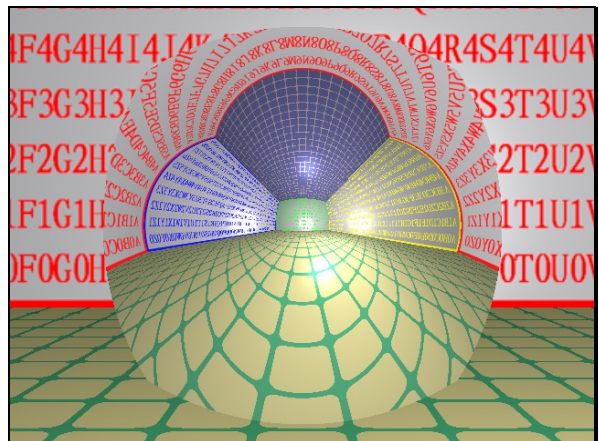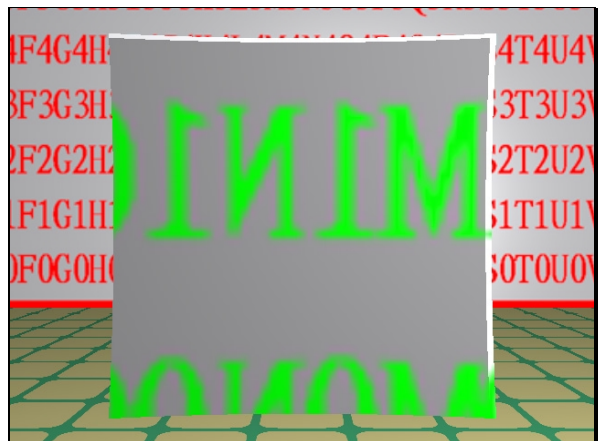
(a)
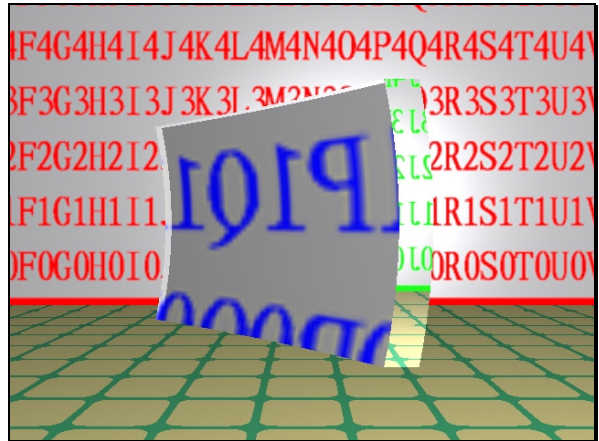
(a)

(b)

(b)

(c)

(c)

Figure 5: *A glass cube is moving (a) laterally from left to right at 99% of the speed of light (b) toward the observer at 90% of the speed of light (c) away from the observer at 99% of the speed of light.*

Figure 6: *A polished metal cube is moving (a) laterally from left to right at 99% of the speed of light (b) towards the observer at 90% of the speed of light (c) away from the observer at 99% of the speed of light.*